Crimson Publishers
Wings to the Research

Research Article

Supercritical Fluid Particle Design for Bionic Inhalation Crystalline Microspheres of Budesonide-Based Series

Yongda Sun[1,2]*

[1]3S PharmaTech LLC, CA, USA

[2]3S PharmaEng Co., Ltd, Shenzhen, China

ISSN: 2576-9170

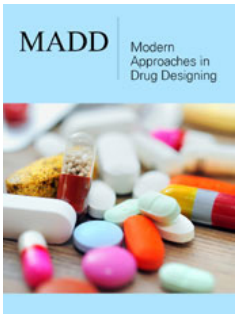

***Corresponding author:** Yongda Sun, PharmaTech LLC, CA, USA and 3S PharmaEng Co., Ltd, Shenzhen, China

Submission: September 10, 2025
Published: October 01, 2025

Volume 4 - Issue 5

How to cite this article: Yongda Sun*. Supercritical Fluid Particle Design for Bionic Inhalation Crystalline Microspheres of Budesonide-Based Series. Mod Appro Drug Des. 4(5). MADD. 000596. 2025.
DOI: 10.31031/MADD.2025.04.000596

Abstract

Particle agglomeration is a major challenge to enhance inhaled drug deposition into the lungs. Current inhalants either use drug-loaded lactose or "soft agglomerated spheroids" or "co-suspended spheres" to address it, not solved the problem at the source. Novel technologies should be introduced to fundamentally tackle it. Supercritical fluid particle design is such new technology. Using the 3S-improved supercritical anti-solvent process, bionic inhalation crystalline microspheres of budesonide-based series were obtained for the first time, and successful in the trial production, including single-component (budesonide), dual-component (budesonide/formoterol) and triple-component (budesonide/glycopyrrolate/formoterol) formulas. They look like red blood cells, and their unique bionic texture was observed and disclosed here for the first time under a high-resolution scanning electron microscope, their surfaces are covered with dense nanowhiskers, while the underlying self-similar ring-like intertwined texture. Such "nano-in-micro" structure make them lightweight, hydrophobic, tough, self-lubricating, with minimal aggregation, excellent dispersion and aerodynamic performance, outstanding results in the *in vitro* carrier-free inhalation assessments. They allow directly inhaled without further processing, laying a solid foundation for a new generation of efficient and simplified carrier free inhalant. Further research found that their changes in the morphology and physical properties are synchronously related to the changes in their surface energy. Surface energy profiles intuitively reflect subtle changes in their morphological and physical properties.

Keywords: Supercritical fluid particle design; Bionic inhalation crystalline microsphere; "Nano in micro" structure; Carrier free inhalant; Surface energy

Introduction

Budesonide (BUD) is a blockbuster drug for the treatment of asthma and Chronic Obstructive Pulmonary Disease (COPD). AstraZeneca has successfully lunched a series inhalation product of budesonide-based, including spray inhalation suspension, Dry Powder Inhaler (DPI), and Pressurized Metered-Dose Inhaler (pMDI). The well-known brands include budesonide suspension for inhalation Pulmicort® Respules®, single-component budesonide Pulmicort® Turbuhaler®, and the combination budesonide/formoterol Symbicort® Turbuhaler® and triple budesonide/glycopyrronium/formoterol Breztri®Aerospheres®. All of them use milled budesonide particles as the main component and do not use lactose particles as carriers. Pulmicort® Turbuhaler® and Symbicort® Turbuhaler® are made into "soft agglomerated spheroids" [1], while Breztri®Aerospheres® is made into "co-suspension spheres"[2], and administered through dedicated inhalers, with a higher lung deposition rate than other inhalation products [3]. It is well known that the efficacy of inhalants depends on interdependent aspects [4]: the formulation, the drug dispensing and packaging (μg scale), the inhaler with dose metering systems, correct usage through patient training and compliance with regulatory frameworks.

Therefore, the small inhaled particles are a big challenge, which means that they have to meet the basic requirements for inhaler to facilitate reproducible dose measuring and good emptying of the dose compartment during inhalation, then, the drug particles should be deposit effectively into the deep lungs. As viewed from inhaled particles, the key is the aerodynamic performance, generally described by fine particle fraction $FPF_{<5\mu m}$, which means the particle proportion with aerodynamic diameter D_a<5μm of the deposition into the deep lungs. However, such drug particles have a high surface energy and tend to agglomerate or adhere to any surface they encounter to reduce surface energy. To overcome this drawback, one approach is to mix with 60-90μm carrier lactose particles [5], the drug particles adhere to the lactose surface to increase dispersion and lung deposition during inhalation, and to achieve microgram dose aliquots during the manufacturing process; other approach is to make "soft agglomeration spheres" with a diameter of several hundred microns from drug particles , or to make "co-suspension microspheres" using low-density porous phospholipid microspheres with drug particles, which are then administered with specially designed inhalers. However, all such methods are quite complex and pose a high barrier to entry for generic inhalant production.

From the perspective of pharmaceutical formulation, drug particle agglomeration is inevitable, with the root cause being the high and uneven surface energy, naturally leading to agglomeration and lower lung deposition rate, which is the greatest challenge in developing "ideal" inhalation products [6]. How to fix this problem?

The direct solution from the source is to be able to produce drug particles with minimal agglomeration. In fact, the Improved Supercritical Antisolvent technology (3S-iSAS) developed by 3S PharmaTech and 3S PharmaEng, which adopts Supercritical Fluid Particle Design (SCF PD) to produce inhaled drug particles with low surface energy profile and minimal agglomeration. After more than a decade of efforts, recombinant human insulin inhalation microspheres [7,8], and especially the bionic inhalation crystalline

microspheres of budesonide-based series (BICM-BUDs) have been successively developed, including BICM-B (budesonide), "Two-in-one" BICM-BF (budesonide and formoterol), and "Three-in-one" BICM-BGF (budesonide/glycopyrronium/formoterol). They have minimal agglomeration, excellent dispersibility, aerodynamic performance, batch consistency, and stability at room temperature. For *in vitro* carrier-free inhalation evaluations, the lung deposition rate of BICM-B has exceeded that of the marketed Pulmicort®.

This study leverages the innovative strategy of "killing three birds with one stone" to develop the SCF PD platform of BICM-BUDs to enable efficient inhalation drug delivery with three key objectives: to combine multiple drugs into bionic microspheres, to simplify preparation into a single-step process, and to enhance drug deposition deep in the lungs. The entire strategy is implemented in three steps. The first is the creation of BICM-B, its characterization and *in vitro* carrier-free inhalation evaluation; The second is to develop BICM-BF, focusing on the applicability of the BICM-B process and the invariance of the product's dual-drug ratio; The third is the development of BICM-BGF, focusing on its unique bionic structure and function, and exploring the close relationship between surface energy and morphology and physical properties.

SCF PD

SCF PD is a new technology for producing nano and micron particles [9-12]. Under supercritical conditions, the drug solution is mixed with CO_2 and atomized through a nozzle to instantly form drug particles with excellent control over physical properties such as particle size, morphology, crystal form, crystal habit, surface energy, and surface charge. Composite particles with unique functional structures, such as co-crystals, salt formation, coated, porous, and uniformly dispersed drug particles, can also be produced by one-step process of the drug solution and excipient solution together, and be used in various Drug Delivery Systems (DDS), such as solubilization, controlled release, sustained release, taste masking, targeting, transdermal, carrier free inhalation, long-acting injectable microspheres, and suspension eye drops, becoming a green "root" technology platform for the production of various new medicines [13-19].

Since Krukonis [20] proposed the concept of drug nucleation in Supercritical CO_2($ScCO_2$), SCF PD has undergone more than 40 years of development, with various technologies emerging one after another. According to the solubility of drugs in $ScCO_2$, the main technologies can be divided into two categories. When a drug can dissolve in $scCO_2$, technologies such as Rapid Expansion of Supercritical Solution (RESS) [21,22] should be used to create solvent-free particles. However, most drugs do not dissolve in $scCO_2$ and can only employ techniques like Supercritical Anti-Solvent (SAS) [23,24], where the drug is first made into a solution that is not soluble in $scCO_2$, then atomized through a nozzle to form drug particles with various functional structures.

In order to produce inhaled particles with low surface energy characteristics and minimal aggregation, the 3S-iSAS technology has made innovative improvements in both apparatus and processes. The innovative improvements of the 3S-iSAS apparatus include the addition of a co-solvent input channel and an imping jet nozzle, optimizing the aspect ratio of the particle formation vessel, as shown in Figure 1.

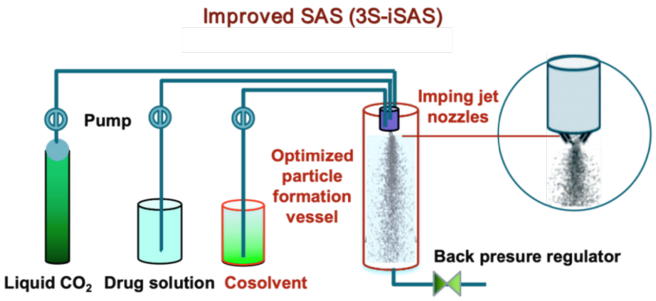

Figure 1: The schematic diagram of the innovative improvements in the 3S-iSAS apparatus.

Both the experimental results and the Computational Fluid Dynamics (CFD) simulations [25] confirmed that the expected

outcomes have indeed been achieved. As shown in Figure 2, the turbulent eddy region rises from the bottom to the top and is confined to the flow area near the nozzle. Therefore, large turbulent eddies disappear, preventing particles from getting trapped, which leads to an increase in particle size causing collisions, adhesion, deformation, and fragmentation, at the same time, many small turbulent eddies emerge, aiding in the formation of BICM-BUDs. In addition, the time streamlines showing particle trajectories are parallel to the vessel wall, allowing the formed drug particles to reach the bottom in the shortest time, resulting in a uniform and narrower particle size distribution.

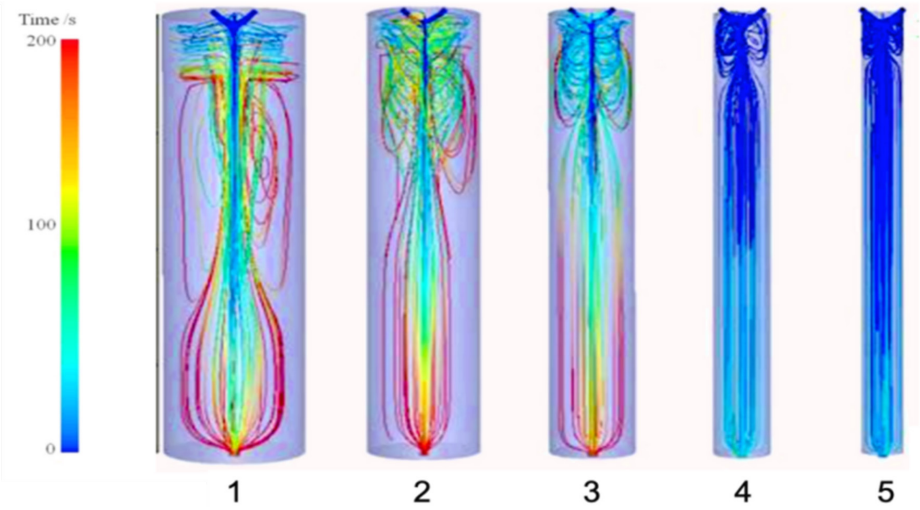

Figure 2: The CFD simulations of the 3S-iSAS apparatus improvements show that the turbulent eddy region rises from the bottom to the top and is confined to the flow region near the nozzle. Also, the time streamline that shows the particle trajectory is parallel to the vessel wall, reaching its bottom in the shortest amount of time.

In terms of the innovative improvements of the process, based on the mechanism of drug particle formation in $ScCO_2$ and a large amount of production experimental data, four proprietary routes of 3S-iSAS process have been established to achieve the company's vision of making "small and smart particles for super drugs", as shown in Figure 3.

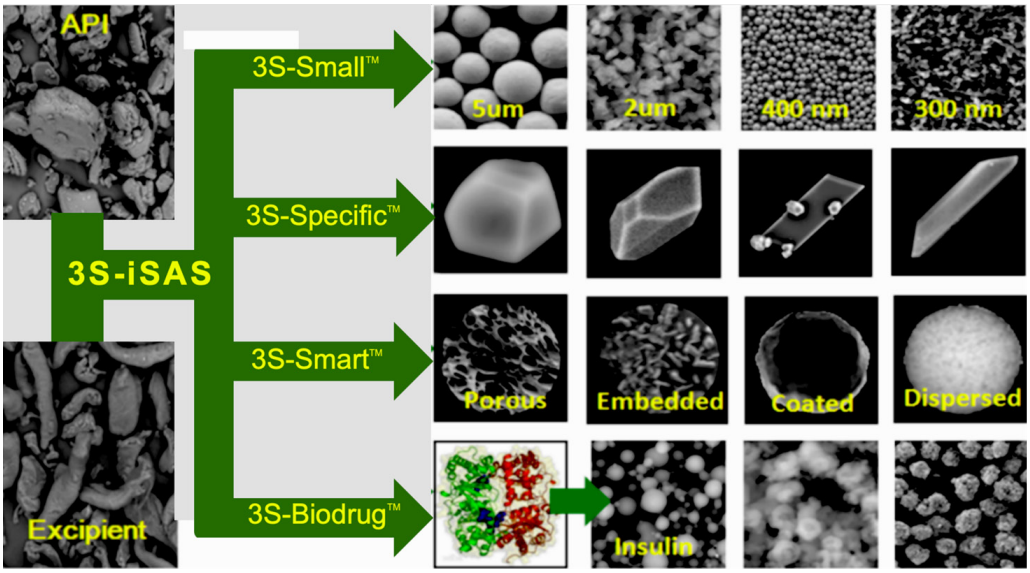

Figure 3: The four proprietary routes of 3S-iSAS process for the development and production of various upmarket drug formulation particles.

A. **3S-Small™ (nano-micron particles)**: used for producing nano-micron drug particles, achieving solubilization, rapid release, inhalation, suspension, and transdermal drug delivery.

B. **3S-Specific™ (polymorphic or crystal habit particles):** used for enhancing polymorph screen, tailoring polycrystalline and habit, preparation of optimized crystal forms or seeds.

C. **3S-Smart™ (composite particles):** used for improving dissolution, permeability, unpalatable taste or release rate by modifying physicochemical properties of particle surface or creation of composite or co-crystal particles.

D. **3S-Biodrug™ (bio-drug particles):** used for long-term potentiating of activity of bio-therapeutics (e.g. proteins, peptides and vaccines) for enhanced delivery of DPI inhalation, injection or transdermal administration.

Material and Methods

Chemicals and reagents

In terms of API, budesonide with a purity of 99.45%, formoterol fumarate with 99.89% and glycopyrrolate with 99.5% were used for the preparation of the solutions used in 3S-iSAS process. All reagents used including acetone, ethanol and methanol were of analytical grade and the liquid CO_2 was of food grade with a purity of 99.9%.

Apparatus of 3S-iSAS

The configuration diagram of the proprietary apparatus of 3S-iSAS shown in Figure 4, which made up of the follow main components: a special designed liquid CO_2 pump with cooler, mass flow meter and electric heat exchanger for preheating the CO_2 to bring the temperature in the particle formation vessel to the required level rapidly, two HPLC pumps of BUDs solution and modifying cosolvent, a particle formation vessel and an imping jet nozzle at the vessel top within a temperature control oven, a back pressure regulator, a cyclone separator. The flow rate of gaseous CO_2 was measured by a rotameter. Temperature and pressure conditions were measured with instruments directly connected to the precipitation vessel, with accuracy of ±0.1 °C and ±0.1MPa, respectively. By manipulating the process conditions of pressure, temperature, solution concentration and flow rate ratio of solution and $ScCO_2$, it is possible to tailor the size, morphology and surface properties of the formed BICM-BUDs [26-28].

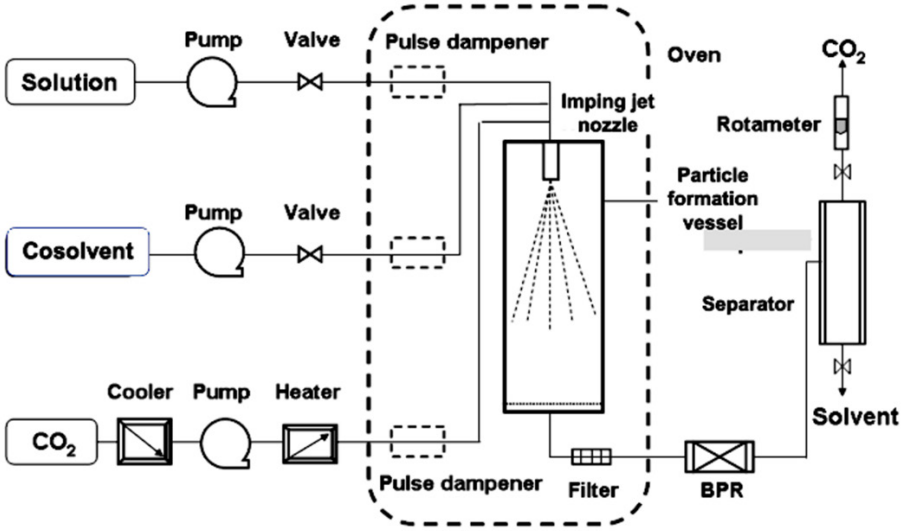

Figure 4: The configuration diagram of the 3S-iSAS proprietary apparatus.

This configuration was different from published SAS apparatus. In brief, the flows of CO_2 and drug solution were solely or discretely pumped into the vessel in SAS which not fully use the jet turbulence energy. The advantages of 3S-iSAS apparatus are that the imping jet nozzle with small orifice from 50μm to 200 μm and the liquid CO_2 pump with high flow rate up to 200ml/min as well as the particle formation vessel with volumes from 100ml to 1000ml (pilot scale) could be assembled multi-configurations and offered stronger jet turbulent pattern to tailor the particle formation. The stream of $ScCO_2$ and BUDs solution are simultaneously pumped into the particle formation vessel through the imping jet nozzle coming into being the turbulent jet of mixtures and leading to nucleation and precipitation due to phase separation and supersaturation of the solute in $ScCO_2$. Particle size and surface properties of the formed particles could be finely tailored by means of the process parameter optimization.

Preparation of BICM-BUDs

BICM-BUDs were prepared by the proprietary 3S-iSAS apparatus. The nature of the organic solvent and the solubility of BUDs in solvent and $ScCO_2$ are important parameters for tailoring the formed particle morphology and ensuring the balanced process. After initial experimental searches with different solvents, the solution of BUDs in acetone was finally selected in this study. The most suitable run conditions were at the pressure between 9-11MPa and temperature at 45-55 °C, the concentration of the BUDs solution about 0.5-1.0% (w/v). In such conditions, the particle size of formed BICM-BUDs was reduced to below the 5μm, no significant particle growth over long processing period. The surface morphology and physical property of the resulting BICM-BUDs can be finely tailored by other parameters, especially sensitive to the flow rate ratio of the solution to $ScCO_2$. In addition, the following operation is stable over long process cycles with

yields of more than 90%: $ScCO_2$ and BUDs solutions are sprayed into the vessel by nozzles. Small droplets of solution were extracted with $ScCO_2$, resulting in supersaturation and crystallization. Rinse with $ScCO_2$ at an appropriate flow rate for 15-20min before the end of each run to dry the BICM-BUDs and remove residual acetone. Finally, all precipitated BICM-BUDs was recovered from the filter bag inside the vessel.

Characterization of BICM-BUDs

The morphology characterized by SEM images were acquired with a Hitachi S-4800 field emission scanning electron microscope. The crystal structure of the particles was analyzed via X-ray diffraction on a model D8 Discover (Bruker AXS, UK) with a low background silicon mount, and recrystallization and thermal properties were evaluated using a Mettler TA4000 DSC calorimeter. The PSD was measured using a Malvern Mastersizer 2000 (Malvern Instruments Ltd., UK). The bulk density is determined using a graduated cylinder with a volume of $10cm^3$, which is filled with accurately weighed samples and the top is leveled. The ratio of mass to sample volume is the bulk density. The electrostatic charge was determined using a Faraday cage. Surface energy analyses were carried out by a second generation of Inverse Gas Chromatography-Surface Energy Analyzer, iGC-SEA (Surface Measurements System Ltd., London, UK). Residual solvent level (parts per million, ppm) was measured by a Capillary Gas Chromatographic Headspace Analysis (GC-HS). Drug content was carried out by a Waters HPLC with 600E pump, 717 autosampler and 2487 dual absorbance detector as well as Zorbax® HPLC column.

In vitro carrier-free inhalation evaluation of BICM-BUDs

The aerodynamic performance was determined by a seven-stage NGI (MSP, US) equipped with a pre-separator, special adaptor to fit the device mouthpieces. A total of ten doses (160μg/dose) were discharged by a Clickhaler® (Innovata Biomed Ltd., UK) into the NGI per determination and sampled at 60L/min for a total inspiratory volume of 4L. Each determination was carried out triple at room temperature and controlled relative humidity conditions of 40-60%. The results of such test are mainly characterized [29] by the Mass Median Aerodynamic Diameter (MMAD), fine particle fraction ($FPF_{<5\mu m}$) and the Geometric Standard Deviation (GSD), which indicates the magnitude of dispersity from the MMAD value.

Stability assessment of BICM-BUDs

Solid-state stability assessments were conducted using the conditions of temperature and humidity recommended in the ICH protocol [30] for long-term testing. The samples were placed in open jars in a glass chamber containing a saturated solution of NaBr to maintain a constant relative humidity of 60%. The glass chamber was stored at 25 °C. At appropriate time intervals, a sample of each powder was removed from the oven for subsequent analysis. The physical stability was assessed using SEM, XRD and DSC and the PSD was measured using a Malvern Mastersizer 2000.

Result and Discussion

BICM-B

There are three types of budesonide crystalline particles without any additives made by 3S-iSAS process, their preparations are not detailed again here, please refer to the original research paper "Carrier free inhaled dry powder of budesonide tailored by supercritical fluid particle design" [31]. Their crystal characteristics are distinct: BUD1 looks like ultrafine diamonds, with a smooth surface and sharp edges; BUD2 nearly spherical particles with rounded surface and uniform particle size; BUD3 resembles red blood cells with thick edges and concave centers. Figure 5 shows SEM images of them compared to the milled budesonide particles (Milled) which used in the inhalation products of budesonide based series by AstraZeneca. Milled exhibits highly irregular particles containing aggregates of ultra-fine amorphous particles. The high-resolution SEM image of BUD3 (Figure 6) clearly shows that they resemble red blood cell-like morphology with biconcave flat sphere, thicker at the edges and thinner at the center. Therefore, named Bionic Inhalation Crystalline Microspheres of Budesonide (BICM-B).

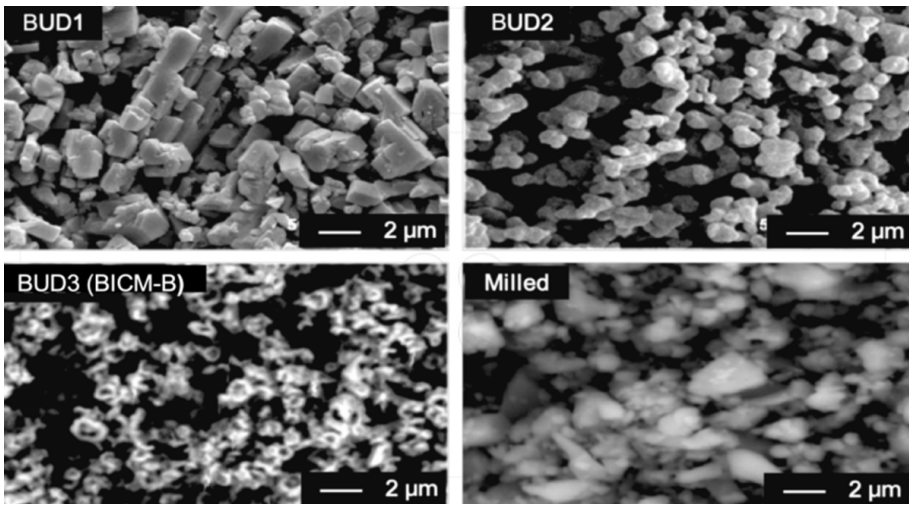

Figure 5: SEM images for three kinds of budesonide's crystalline particles made by 3S-iSAS process.vs Milled budesonide.

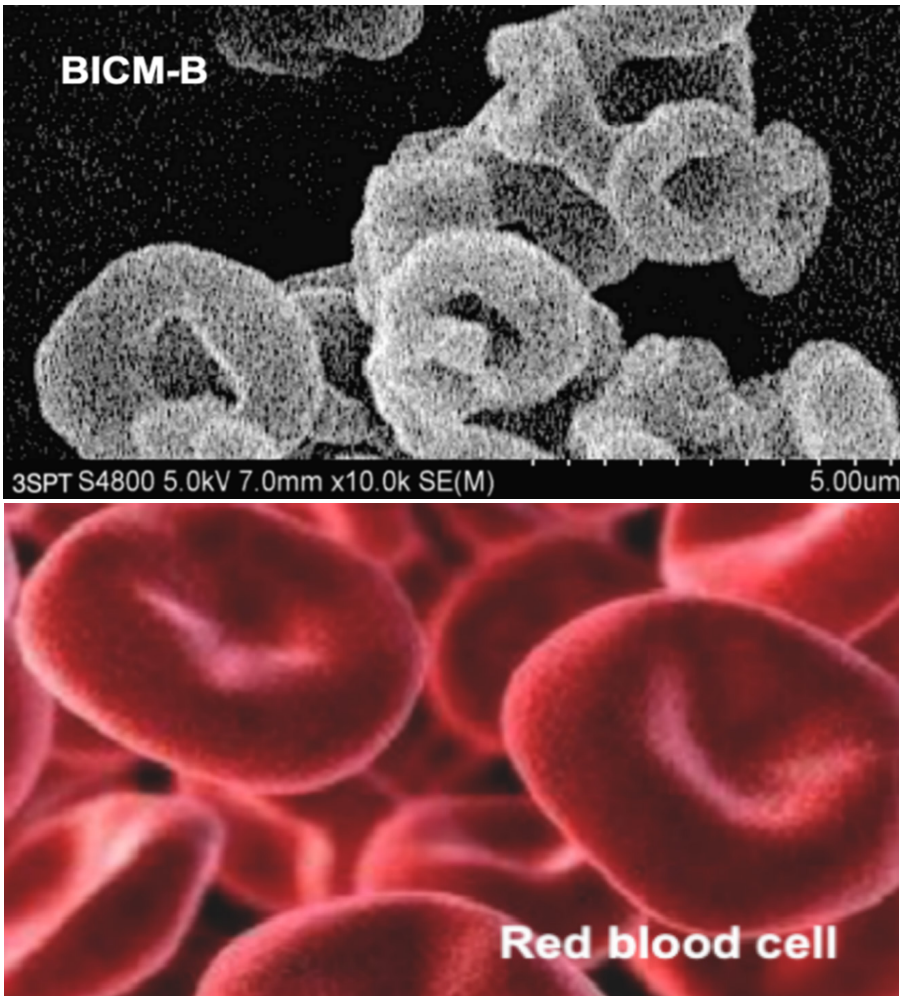

Figure 6: The high-resolution SEM image of BICM-B (the top) clearly shows that their morphology resembles the red blood cells (the bottom).

BICM-B is typical crystalline conformed by XRD patterns, the peak positions and relative intensities were consistent with API, indicated that there were no changes in crystal structure after 3S-iSAS process. the melting point is 258.7 °C confirmed by DSC analysis that is in a good agreement with API and the observation of Velaga et al. [32]. BICM-B's physical properties are particularly significant in comparison with Milled (Table 1). Its Particle Size Distribution (PSD) is narrowly normal, with D_{10}=1.08μm, D_{50}=1.93μm, D_{90}=3.68μm, and the proportion of 94% for particles between 1-5μm. Its bulk density is very low, at only 0.06g/cm^3, close to the values reported in reference [33]. The residual solvent content is as low as 800ppm. The specific charge reaches -64.9nC/g, which is beneficial for increasing the deposition rate in the lungs upon inhalation, as confirmed by studies using physical lung models [34], animal experiments [35], and research on human volunteers [36,37].

Table 1: The physical properties of BICM-B vs Milled.

ID of BUD Particles		BICM-B	Milled
Morphology		Red blood cell like	Irregular
Crystallinity (%)		100	<100
Melting point (C°)		258.7	258.7
PSD data	D_{10} (μm)	1.08	0.81
	D_{50} (μm)	1.93	2.12
	D_{90} (μm)	3.68	4.95
	1-5μm particles	94%	75%
Bulk density (g/cm^3)		0.06	0.32

Specific Charg (nC/g)		-64.9	-1.96
Residual solvent (ppm)		828	2563
Stability at RT (year)		>2	2
NGI data	FPF<5μm (%)	32.9	7.33
	MMAD (μm)	4.68	4.65
	GSD	1.89	2.14

The aggregation behavior of the particles can be observed directly. As shown in Figure 7, there is no visible aggregation in BICM-B, while the crushed particles aggregate quite significantly, with many clusters clearly visible, despite the fact that the PSD of the two types are almost the same. Even BICM-B made by 3S-iSAS pilot scale process shows no signs of agglomeration in the SEM image of Figure 8. Another way for visualization of the particle agglomeration degree is to utilise Pressure Titration Curves (PTC) to characterise particle cohesivity and ease of de-agglomeration [38,39]. The particles of BICM-B or Milled were sequentially subjected to dispersing pressures of 1-5 bar in the Sympatec HELOS/RODOS laser diffractometer and particle size distribution curve measurements were recorded. The various types of PTC reveal different degrees of agglomeration of particles.

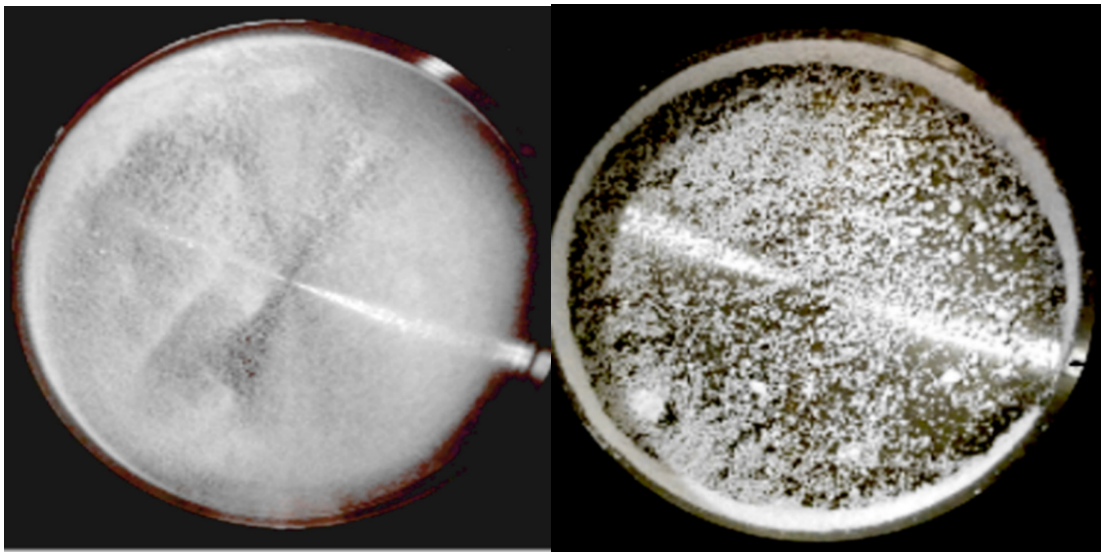

Figure 7: Comparison of aggregation behaviour of BICM-B vs Milled, there is no visible aggregation in BICM-B (left), while the crushed particles aggregate clearly visible in Milled (right).

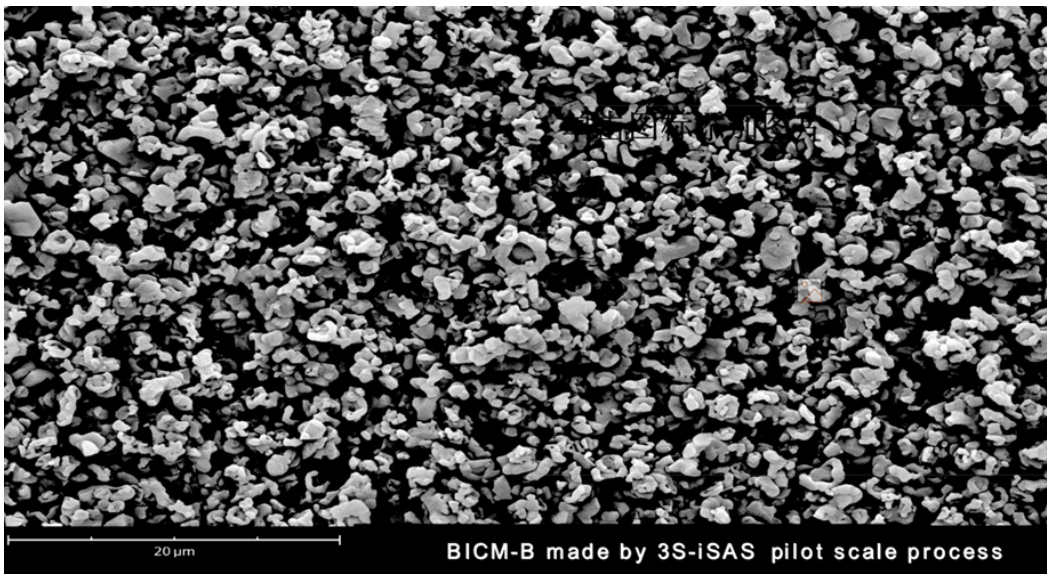

Figure 8: The SEM image of BICM-B made by 3S-iSAS pilot scale process.

Now, let's compare the PTC of BICM-B vs Milled (Figure 9). BICM-B shifted almost completely parallel towards smaller particle sizes by the same distance. This means that regardless of the size of the particle, the agglomeration force and the de-agglomeration effect on them is almost the same. Milled shows a clear difference, only shifting a little towards smaller particle sizes in the middle part, and the particles at both ends barely shifting, which means that the particles with different sizes have different agglomeration forces, at both ends of the PTC have greater agglomeration forces and poor de-agglomeration effect. BICM-B's aerodynamic performance was significantly enhanced due to rare aggregation. The most critical data for *in vitro* carrier-free inhalation evaluation, $FPF_{<5\mu m}$, shown in Figure 10, BICM-B at 32.9%, exceeding Pulmicortr® at 28.4% [40], which is very close to the published value of 29.8% determined from *in vitro* tests using gamma scintigraphy at the same flow rate [41]. Although the PSD of Milled is very close to that of BICM-B (Table 1), there is still a significant gap for *in vitro* carrier-free inhalation evaluation, where Milled shows $FPF_{<5\mu m}$ at 7.33% due to severe aggregation.

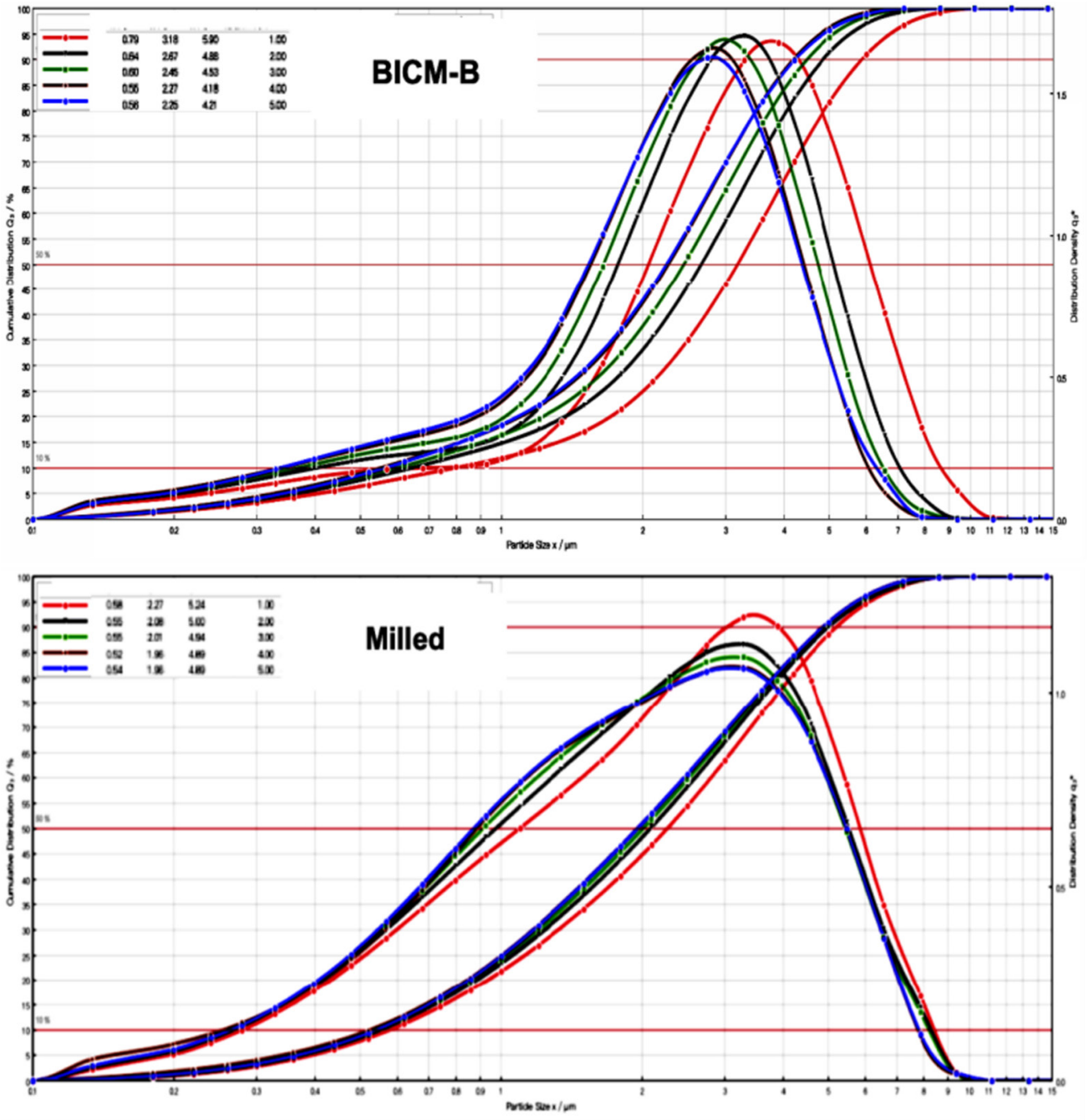

Figure 9: Comparison of the PTC of BICM-B vs Milled. When the dispersing pressure is sequentially increased from 1 to 5 bar, BICM-B shifted almost completely parallel towards smaller particle sizes by some distance. But, Milled, only the middle parts shift slightly towards smaller particle sizes, five curves almost entangled together.

The excellent dispersion and very low agglomeration of BICM-B can be seen at a glance by analyzing the percentage of particles retained at each NGI stage in Figure 10. The drug particles were inhaled under a standard airflow of 60L/min, and the cut-off particle size from P to MOC was 10.0, 0.806, 4.46, 2.82, 1.66, 0.94, 0.55, 0.34,0μm respectively. Among the A, T and P stages, the P stage has the most drug particles retained, with Milied up to 72%, Pulmicort® 40%, and BICM-B only 20%. This means that BICM-B is the least agglomerated during inhalation. In addition, the percentage of $FPF_{<1\mu m}$ is also worth paying attention to. The cut-off particle size of the S5 stage is 0.94μm, and the percentage of cumulative particles retained in the subsequent stages defines as $FPF_{<0.94\mu m}$, here Pulmicort®, at 4%, BICM-B close to 0. Considering that in therapeutic practice, most of the fine particles of 0.1-1μm is exhaled from the body [42], removing the contribution of $FPF_{<0.94\mu m}$, the $FPF_{<5\mu m}$ of Pulmicort® becomes 24.2%, while the $FPF_{<5\mu m}$ of BICM-B is almost unchanged and is still close to 32.9%. These data confirm that BICM-B can not only be directly inhaled without additional handling but also has an extremely simple production, manufactured by a single step of the 3S-iSAS process.

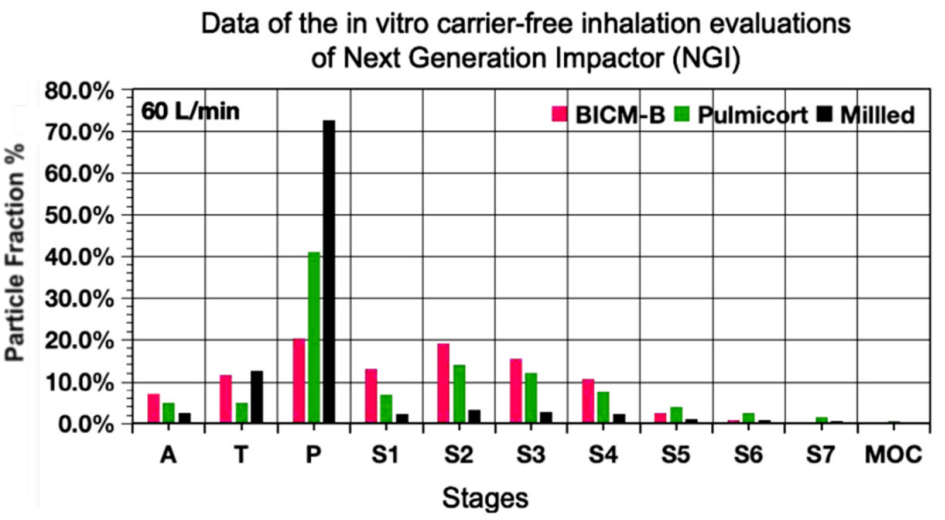

Figure 10: The most critical data for *in vitro* carrier-free inhalation evaluation by NGI, $FPF_{<5\mu m}$, shows BICM-B at 32.9%, exceeding Pulmicortr® at 28.4%, where Milled shows $FPF_{<5\mu m}$ at 7.33% due to severe aggregation.

BICM-BF

The successful trial production of BICM-BF is based on the experience of BICM-B. In the formulation of Symbicort®, the mass ratio of budesonide to formoterol is 80/4.5 or 160/4.5, which varies widely. Therefore, the development of BICM-BF faced two new challenges: (1) Can it be made into BICM-BF? (2) Can the product still maintain the mass ratio of the two drugs?

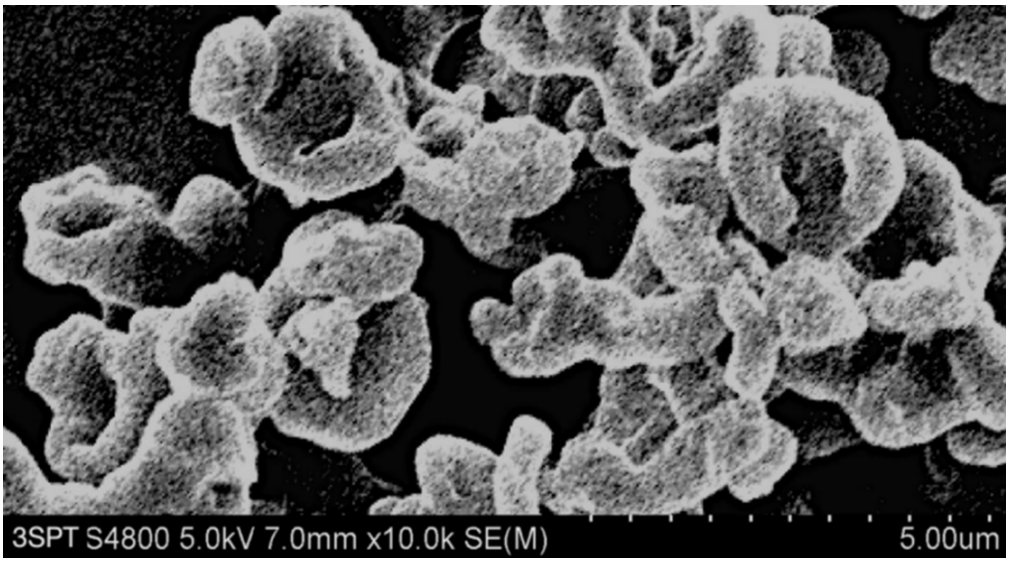

Figure 11: The high-resolution SEM images of BICM-BF made by 3S-iSAS process, which clearly shows that their morphology resembles the red blood cells.

Using the 3S-iSAS process with a 160/4.5 feed mass ratio, the pilot results were as follows: (1) The process for preparing BICM-B was still applicable when a very small amount of formoterol was added to a large amount of budesonide. The high-resolution SEM images of the BICM-BF are shown in Figure 11. It still has a nice red blood cell-like shape, PSD with good normality of D_{10}=0.82μm, D_{50}=2.61μm, and D_{90}=4.83μm. the data of XRD and DSC confirmed that its crystallinity is up to standard. (2) The mass ratio of the two drugs in the BICM-BF still was unchanged, more details seeing the Table 2. Because the drugs in suitable solvent were mixed by the molecular level, and no any components were lost during the 3S-iSAS process. Also, the solvent residue in the product was reduced to 968 ppm, far below the requirements of the pharmacopoeia. BICM-BF completely avoids the complex process such as preparing Symbicort® and ensures the consistency of the drug mass ratio in each dose. Through *in vitro* carrier-free inhalation evaluations, its $FPF_{<5\mu m}$=30.1%. Moreover, the product has a stability period of over two years at room temperature. This opens up a simplified and straightforward path for the development of multi-component drug combination inhalation dry powders.

Table 2: The design objects and results of BICM-BF by 3S-iSAS process.

BICM-BF	Design Objects	Results
Yield (%)	>85	>90
Crystal form	Consistent with API	Consistent with API
Mass ratio of B/F	160/4.5=35.56	35.55±0.02
PSD (μm)	D_{50} ≤3 D_{90} ≤5	D_{50}=2.43 D_{90}=4.56
Particle shape	BICM	BICM
Solvent residue (ppm)	≤2000	968
Stability at RT (year)	≥2	>2

BICM-BGF

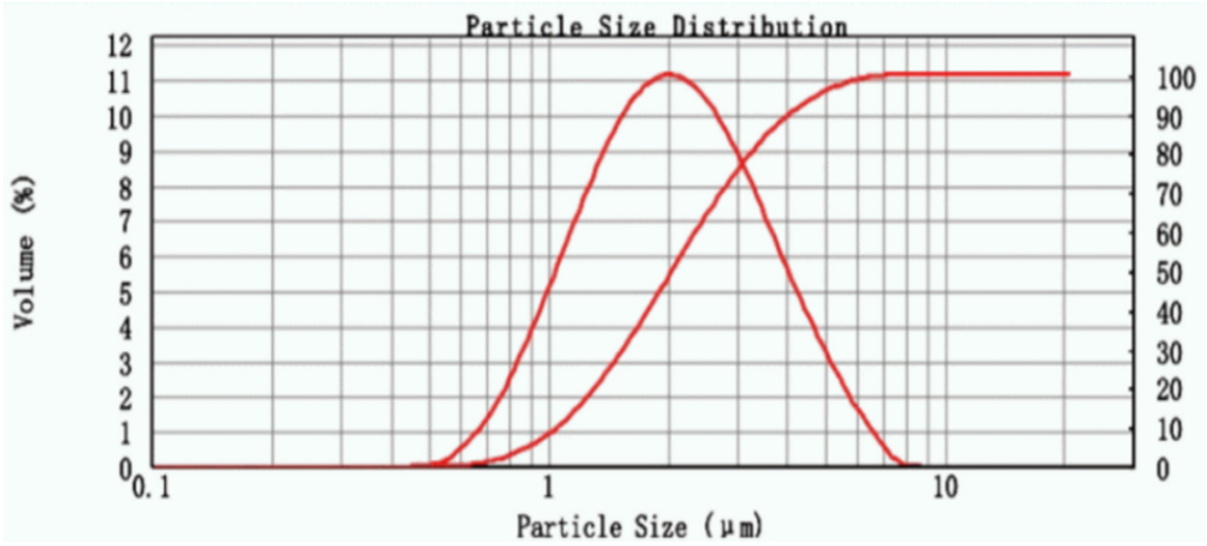

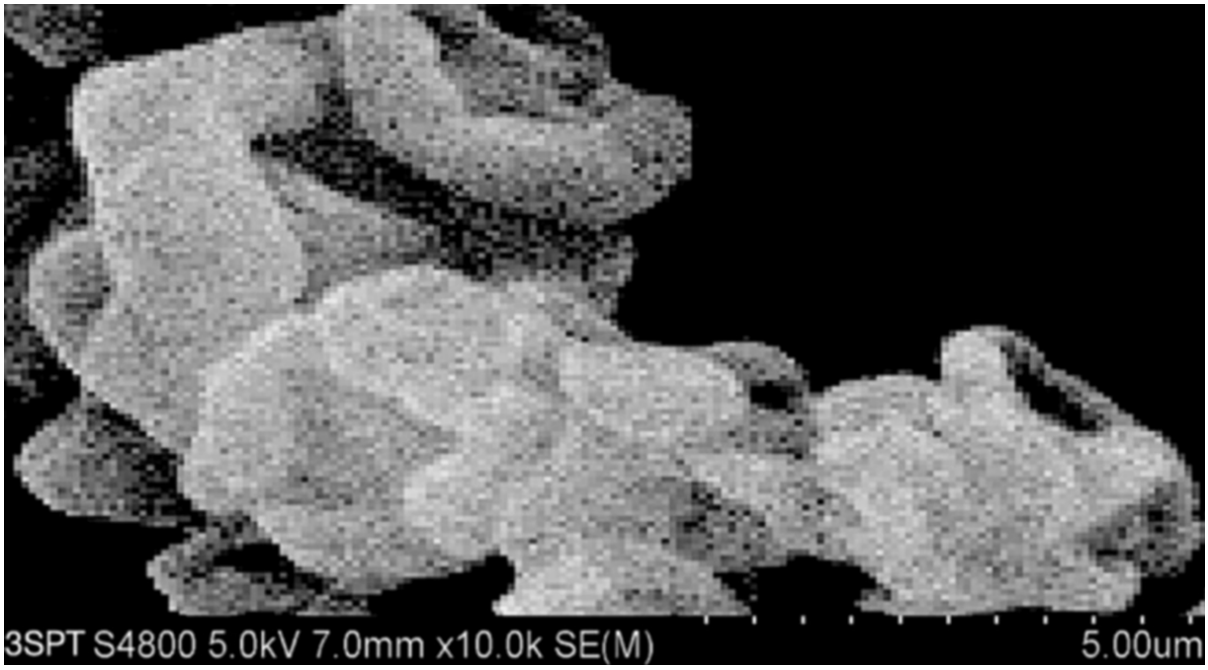

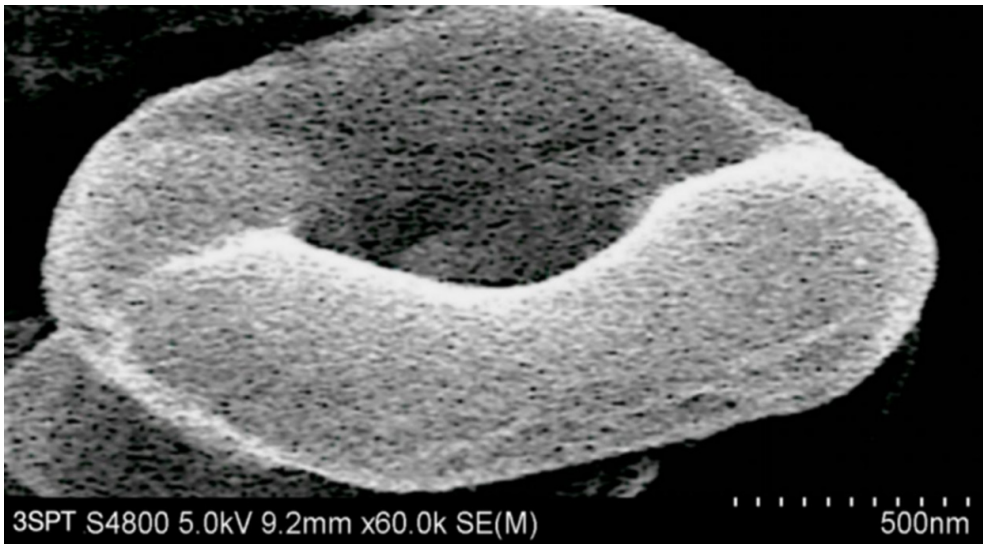

Figure 12: The PSD and high-resolution SEM images of BICM-BGF made by 3S-iSAS process. The top curve shows its PSD with nice normality of D_{10}= 1.06μm D_{50}= 2.06μm, D_{90}= 4.09μm, and 85.6% of 1-5μm particles; the middle SEM showing that they resemble red blood cells; while the bottom SEM is a high magnification image, showing clearly the unique "nano-in-micro" structured bionic texture: the surface has dense felt-like nanowhiskers, and underneath it is a looming ring-like interwoven texture.

The mass ratio of budesonide/glycopyrrolate/formoterol in the formulation of Breztri®Aerospheres® is 160/9/4.5 or 160/7.2/4.5. Referring to the preparation process of BICM-BF, the three drugs were mixed and dissolved into a solvent according to the formulation ratio, and then sprayed into the particle forming vessel together with $ScCO_2$ to instantly produce BICM-BGF with suitable particle size and physical properties. Because the three drugs are homogeneously mixed at the molecular level, the composition of BICM-BGF is consistent with the formulation. They resemble red blood cells, and with excellent crystallinity, dispersion and aerodynamic performance. The data of XRD and DSC confirmed that its crystallinity is up to standard. Its PSD with nice normality of D_{10}= 1.06μm,D_{50}= 2.06μm, D_{90}= 4.09μm, and 85.6% of 1-5μm particles, as shown in Figure 12.

BICM-BGF has a unique "nano-in-micro" structured bionic texture: its surface is not smooth, but rather hairy, with self-similar ring-like intertwined texture structures hidden beneath the dense felt-like nanowhiskers [43], as shown in Figure 12. Such "nano-in-micro" structure (1) increases the specific surface area and structural toughness, reduces the bulk density, and facilitate the precise dispensing of dosage of formulation; (2) minimizes agglomeration viscosity and frictional resistance [44], which is conducive to improving fluidity and aerodynamic properties; (3) enhances hydrophobicity [45] and stability, which is conducive to long-term storage at room temperature. In short, this self-lubricating property gives it very good aerodynamic performance and the physical basis for its leading position in the *in vitro* carrier-free inhalation evaluation.

Surface Energy

As mentioned in the section of BICM-B, the good aerodynamic performance is derived from its various outstanding physical properties. So, is it possible to encompass and characterize them by a single physical quantity with a higher dimension? The surface energy of powder is such a physical quantity that encompasses and maps the surface morphology and physical properties of the powder, both are closely related and mapped to each other. Even the smallest differences in the surface morphology and physical properties of particles can be detected and recognized by surface energy, such as changes in surface roughness, surface charge, friction, fluidity, hygroscopicity and stability. The specific surface energy or work related to surface morphology and physical properties can be measured to identify them. In general, powder with low and gentle surface energy profile correspond to higher crystallinity, stronger hydrophobicity, lower viscosity and good stability; powder with high and steep surface energy profile have lower crystallinity, stronger hydrophilicity, higher viscosity, and poorer stability [46].

Let's start by looking at the total surface energy profiles of BICM vs Milled, as shown in Figure 13, BICM's is low and flat, which means that the particles of BICM-B are at almost the same energy level regardless of size and therefore are not prone to agglomeration; Milled's is high and steep, which means that its energy level distribution is very different, with a natural tendency to move into a more stable low-energy state through agglomeration. In terms of the maximum value of the total surface energy (Table 3), BICM-B at 48.90mJ/m^2 and Mellied at 77.61mJ/m^2. This decrease of 28.71mJ/m^2 in energy reflects various changes in the morphological and physical properties of BICM-B vs Milled, such as changes in surface morphology, increases in crystallinity, specific surface area, surface charge, toughness, dispersion, fluidity, and hydrophobicity, and decreases in bulk density, agglomeration, and friction, which are quantitatively characterized by the data in Table 1.

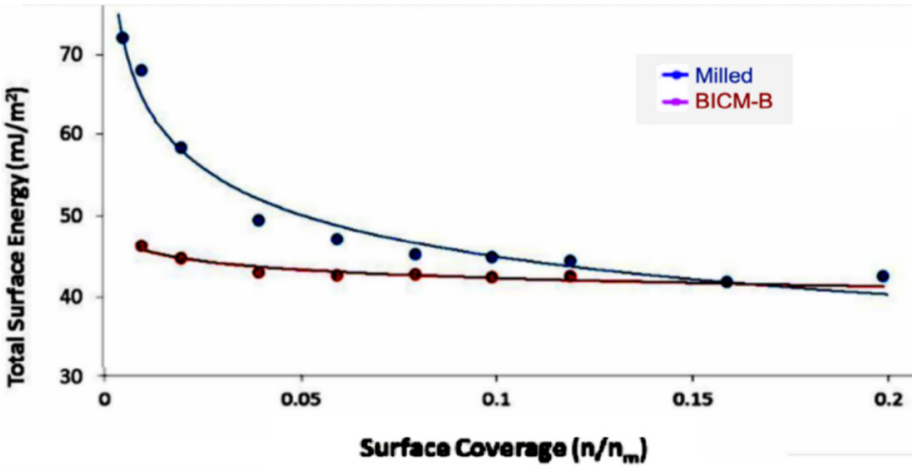

Figure 13: The comparison of the total surface energy profiles (γ_s^T as function of surface coverage) of BICM-B vs Milled, measured by IGC-SEA.

Table 3: The surface energy of BICM-B vs Milled.

γ_s^D - the dispersive component of the surface energy,

γ_s^{AB} - the specific component of the surface energy

γ_s^T - the total surface energy

γ_s^{50} - the median, has been defined as the surface energy where half of the population lies below this value.

ID of Particles	γ_s^D (mJ/m²)	γ_s^{AB} (mJ/m²)	γ_s^T (mJ/m²)
	Min $\gamma_s^{D,50}$ Max	Min $\gamma_s^{AB,50}$ Max	Min $\gamma_s^{T,50}$ Max
Milled	39.88 44.62 65.28	3.27 4.92 12.13	43.28 49.70 77.61
BICM-B	41.79 42.93 47.89	0.43 2.36 3.15	42.51 43.70 48.90

Further studies found that the agglomeration and hydrophobicity of inhalation particles, which are of the greatest concern, can lead to changes in specific work even if they occur slightly. For example, agglomeration and friction of particles are related to the thermodynamic cohesion work $W^{1\text{-}2}_{adh}$, which is the work done to reversibly separate two adsorbed together particles, with a low $W^{1\text{-}2}_{adh}$ indicating low agglomeration adhesion and less frictional resistance. Hygroscopicity is the degree of interaction between a powder sample and water molecules. Using a water molecule probe, the work of adhesion WWadh between the sample and water molecules, is measured, and thus the hygroscopicity is quantitatively characterized. Lower W^{W}_{adh} implies weaker water solubility and less hygroscopicity.

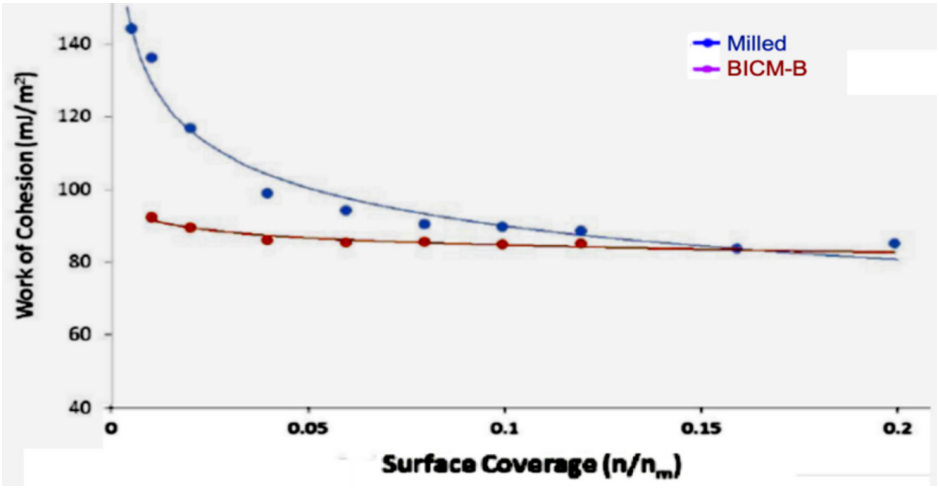

Figure 14: The comparison the cohesion work $W^{1\text{-}2}_{adh}$ ($W^{1\text{-}2}_{adh}$ as function of surface coverage) of BICM-B vs Milled, measured by IGC-SEA.

The data measured by IGC-SEA confirm this close correlation. Figure 14 show the curves of cohesion work W^{1-2}_{adh}, BICM-B is a low and gentle. while Milled is a high and steep. The maximum value of W^{1-2}_{adh}, BICM-B at 92.54mJ/m^2. Milled at 146.68mJ/m^2, there is a reduction of 54.14mJ/m^2, which means low agglomeration adhesion and less frictional resistance in BICM-B. Similarly, the curves of adhesion work W^{W}_{adh}, shown in Figure 15, the maximum value of W^{W}_{adh}, BICM-B at 73.27mJ/m^2, milled at 150.19mJ/m^2, there is a reduction of 76.92mJ/m^2, which means weaker water solubility and less hygroscopicity in BICM-B. Obviously, the changes of the morphology and physical properties of BICM-B vs Milled lead to the corresponding change of total surface energy or specific work, both are closely related and mapped to each other. So, the expression of surface energy and specific work is an overall measure at a higher dimension than data of the morphology and physical properties.

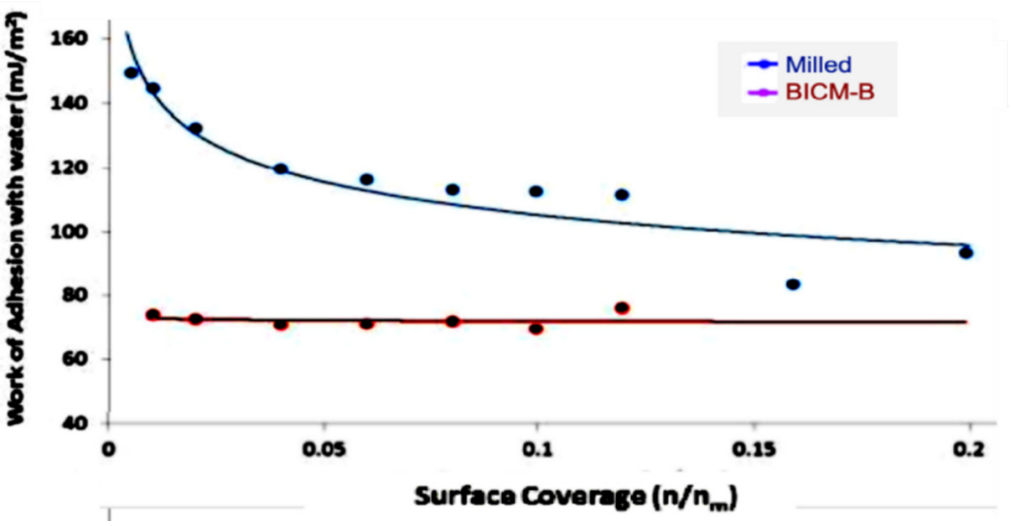

Figure 15: The comparison the cohesion work W^{W}_{adh} (W^{W}_{adh} as function of surface coverage) of BICM-B vs Milled, measured by IGC-SEA.

Conclusion

This study developed a new carrier free inhalation particles manufacturing platform, SCF PD platform of 3S-iSAS process, which produced BICM-BUDs, including single-component (budesonide), dual-component (budesonide/formoterol) and triple-component (budesonide/glycopyrrolate/formoterol) formulas, They possess unique "nano-in-micro" bionic structures: resembling red blood cells, beneath the surface covered with dense nanowhiskers underlying self-similar ring-like intertwined texture, making them lightweight, hydrophobic, tough, self-lubricating, exhibiting minimal aggregation, excellent dispersion and aerodynamic performance. The 3S-iSAS process does simplify the preparation of BICM-BUDs into a one-step operation and does enhance the deposition of the drug in the lungs by carrier free inhalation.

Using surface energy profile to evaluate inhaled powders is a new exploration in this study. This elevates the characterization of the multifaceted phenomena of inhaled powders to the level of physical roots. The surface energy profile of BICM-B is low and flat, resulting in minimal aggregation. In contrast, the surface energy profile of Milled is high and steep, leading to severe aggregation. It can indeed be said that a simple and intuitive surface energy profile distinguishes between the two eras of inhaled powders.

References

1. Healy AM, Amaro MI, Paluch KJ, Tajbe L (2014) Dry powders for oral inhalation free of lactose carrier particles. Advanced Drug Delivery Reviews (75): 32-52.
2. Ferguson GT, Hickey AJ, Dwivedi S (2018) Co-suspension delivery technology in pressurized metered-dose inhalers for multi-drug dosing in the treatment of respiratory diseases. Respiratory Medicine (134): 16-23.
3. Demoly P, Hagedoorn P, De Boer AH, Frijlink HW (2014) The clinical relevance of dry powder inhaler performance for drug delivery. Respiratory Medicine 108(8): 1195-1203.
4. Stegemann S, Kopp S, Borchard G, Shah VP, Senel S, et al. (2013) Developing and advancing dry powder inhalation towards enhanced therapeutics. Eur J Pharm Sci 48(1-2): 181-194.
5. Rahimpour Y, Hamishehkar H (2012) Lactose engineering for better performance in dry powder inhalers. Adv Pharm Bull 2(2): 183-187.
6. Sorino C, Negri S, Spanevello A, Visca D, Scichilone N (2020) Inhalation therapy devices for the treatment of obstructive lung diseases: the history of inhalers towards the ideal inhaler. Eur J Intern Med (75): 15-18.
7. Sun Y (2010) Protein microspheres for pulmonary drug delivery. Frontiers of Chemical Engineering in China 4(1): 82-86.
8. Sun Y (2012) A method for the preparation of human insulin inhalation dry powder using supercritical fluid technology.
9. Tom JW, Debenedetti PG (1991) Particle formation with supercritical fluids-A review. J Aerosol Sci 22(5): 555-584.
10. Jung J, Perrut M (2001) Particle design using supercritical fluids: Literature and patent survey. J Supercritical Fluids 20(3): 179-219.
11. Kompella UB, Koushik K (2001) Preparation of drug delivery systems using supercritical fluid technology. Crit Rev Ther Drug Carr Syst 18(2): 173-199.
12. Reverchon E, Porta GD (2003) Particle design using supercritical fluids. Chemical Engineering & Technology 26(8): 840-845.

13. Sun Y (2014) Supercritical fluid particle design for poorly water-soluble drugs (Review). Current Pharmaceutical Design 20(3): 349-368.

14. Sun Y (2015) Editorial: Particle design of drug delivery system. Current Pharmaceutical Design 21(19): 2514.

15. Sun Y (2015) Supercritical fluid particle design of DPI formulation (Review). Current Pharmaceutical Design 21(19): 2514-2542.

16. Padrela L, Miguel AR, Andreia D, Dias AMA, Mara EMB et al. (2018) Supercritical carbon dioxide-based technologies for the production of drug nanoparticles/nanocrystals-A comprehensive review. Adv Drug Deliv Rev 131: 22-78.

17. Bin LK, Ashok K, Syafiq F, Uddin ABMH, Razak A, et al. (2020) Supercritical fluid technology and its pharmaceutical applications: A revisit with two decades of progress. Indian Journal of Pharmaceutical Education and Research 54(2s): s1-s11.

18. O'Sullivan A, Ryan KM, Padrela L (2022) Production of biopharmaceutical dried-powders using supercritical CO_2 technology. J Supercritical Fluids 187: 105645.

19. Trivedi V, Ajiboye AL (2023) Supercritical fluids: A promising technique in pharmaceutics. In: Lamprou D (Ed.), Nano-and Microfabrication Techniques in Drug Delivery Recent Developments and Future Prospects, Springer, Cham, Switzerland, pp: 295-320.

20. Krukonis VJ (1984) Supercritical fluid nucleation of difficult-to-comminute solids. Annual Meeting, American Institute of Chemical Engineers Journal, San Francisco, USA, pp. 140-149.

21. Türk M, Wahl MA, Hils P, Helfgen B, Schaber K, et al. (2002) Micronization of pharmaceutical substances by the Rapid Expansion of Supercritical Solutions (RESS): A promising method to improve bioavailability of poorly soluble pharmaceutical agents. J Supercritical Fluids 22(1): 75-84.

22. Matson DW, Fulton JL, Peterson RC, Smith RD (1987) Rapid expansion of supercritical fluid solutions: Solute formation of powders, thin films, and fibers. Ind Eng Chem Res 26(11): 2298-2306.

23. Reverchon E, Marco ID, Porta GD (2002) Tailoring of nano-and micro-particles of some superconductor precursors by supercritical antisolvent precipitation. J Supercritical Fluids 23(1): 81-87.

24. Snavely WK, Subramaniam B, Rajewski RA, Defelippis MR (2002) Micronization of insulin from halogenated alcohol solution using supercritical carbon dioxide as an antisolvent. J Pharm Sci 91(9): 2026-2039.

25. Zhang M, Wang Z, Li Y, Geng Z (2013) Research on the influence of diameter of the particle formation vessel in the SAS process. Journal of Computer and Applied Chemistry 30(7): 703-708.

26. De Zordi N, Kikic I, Moneghini M, Solinas D (2012) Solubility of pharmaceutical compounds in supercritical carbon dioxide. J Supercritical Fluids 66: 16-22.

27. Vatanara A, Najafabadi AR, Khajeh M, Yamini Y (2005) Solubility of some inhaled glucocorticoids in supercritical carbon dioxide. J Supercritical Fluids 33(1): 21-25.

28. Chieh-Ming H, Jadran V (2015) Vapor-liquid equilibrium measurements of the binary mixtures CO_2+acetone and CO_2+pentanones. J Supercritical Fluids 100: 160-166.

29. Jaafar-Maalej C, Andrieu V, Elaissari A, Fessi H (2009) Assessment methods of inhaled aerosols: Technical aspects and applications. Expert Opin Drug Deliv 6(9): 941-959.

30. European Medicines Agency (2003) Guideline specification Q1A(R2), Draft, Stability testing of new drug substances and products, ICH (International Conference on Harmonisation).

31. Sun Y (2016) Carrier free inhaled dry powder of budesonide tailored by supercritical fluid particle design. Powder Technology 304: 248-260.

32. Velaga SP, Berger R, Carlfors J (2002) Supercritical fluids crystallization of budesonide and flunisolide. Pharm Res (19): 1564-1571.

33. Jennifer ML, Helena S, Srinivas P, Peter Y, Andy C et al. (2005) SCF-engineered powders for delivery of budesonide from passive DPI devices. Journal of Pharmaceutical Sciences 94(10): 2276-2288.

34. Karner S, Urbanetz NA (2011) The impact of electrostatic charge in pharmaceutical powders with specific focus on inhalation-powders. J Aerosol Sci 42(6): 428-445.

35. Fraser DA (1966) The deposition of unipolar charged particles in the lungs of animals. Arch. Environ Health 13(2): 152-157.

36. Melandri C, Tarroni G, Prodi V, Zaiacomo TD, Formignani M, et al. (1983) Deposition of charged particles in the human airways. J Aerosol Sci 14(5): 657-669.

37. Bailey AG (1997) The inhalation and deposition of charged particles within the human lung. J Electrost 42(1-2): 25-32.

38. Jaffari S, Forbes B, Collins E, Barlow DJ, Martinet GP, et al. (2013) Rapid characterisation of the inherent dispersibility of respirable powders using dry dispersion laser diffraction. International Journal of Pharmaceutics 447(1-2): 124-131.

39. Behara SRB, Larson I, Kippax P, Morton DAV, Stewart P (2011) An approach to characterising the cohesive behaviour of powders using a flow titration aerosolisation based methodology. Chemical Engineering Science 66(8): 1640-1648.

40. Mohanad NS, Yusrida D, Peh KK, Yvonne TFT (2010) Aerodynamic characterization of marketed inhaler dosage forms: High performance liquid chromatography assay method for the determination of budesonide. African Journal of Pharmacy and Pharmacology 4(12): 878-884.

41. Hirst PH, Newman SP, Clark DA, Hertog MGL (2002) Lung deposition of budesonide from the novel dry powder inhaler AirmaxTM. Respiration Medicine 96(6): 389-396.

42. De Boer AH, Gjaltema D, Hagedoorn P, Frijlink HW (2015) Can 'extrafine' dry powder aerosols improve lung deposition? European Journal of Pharmaceutics and Biopharmaceutics 96: 143-151.

43. Singh H, Kumarm V (2021) Cellulosic nanowhiskers: Preparation and drug delivery application. Curr Drug Deliv 18(10): 1426-1434.

44. Puoza JC (2025) Research progress of surface texturing and thermal diffusion technology to improve tribological properties of materials. Progress in Engineering Science 2(1): 100034.

45. Parvate S, Dixit P, Chattopadhyay S (2020) Superhydrophobic surfaces: Insights from theory and experiment. The Journal of Physical Chemistry 124(8): 1323-1360.

46. Williams DR (2015) Particle engineering in pharmaceutical solids processing: Surface energy considerations. Current Pharmaceutical Design 21(19): 2677-2694.